**Article:**

# The structural basis of semantic control: Evidence from individual differences in cortical thickness

Xiuyi Wang[a], Boris C. Bernhardt[b], Theodoros Karapanagiotidis[a], Irene De Caso[a], Tirso Rene del Jesus Gonzalez Alam[a], Zacharria Cotter[a], Jonathan Smallwood[a], Elizabeth Jefferies[a,]

[a] Department of Psychology and York Neuroimaging Centre, University of York, York, United Kingdom

[b] Multimodal Imaging and Connectome Analysis Lab, Montreal Neurological Institute, McGill University, Montreal, QC, Canada

Correspondence to: Xiuyi Wang, Department of Psychology, University of York, YO10 5DD, UK. xw1365@york.ac.uk

## Abstract

Semantic control allows us to shape our conceptual retrieval to suit the circumstances in a flexible way. Tasks requiring semantic control activate a large-scale network including left inferior prefrontal gyrus (IFG) and posterior middle temporal gyrus (pMTG) – this network responds when retrieval is focussed on weak as opposed to dominant associations. However, little is known about the biological basis of individual differences in this cognitive capacity: regions that are commonly activated in task-based fMRI may not relate to variation in controlled retrieval. The current study combined analyses of MRI-based cortical thickness with resting-state fMRI connectivity to identify structural markers of individual differences in semantic control. We found that participants who performed relatively well on tests of controlled semantic retrieval showed increased structural covariance between left pMTG and left anterior middle frontal gyrus (aMFG). This pattern of structural covariance was specific to semantic control and did not predict performance when harder non-semantic judgements were contrasted with easier semantic judgements. The intrinsic functional connectivity of these two regions forming a structural covariance network overlapped with previously-described semantic control regions, including bilateral IFG and intraparietal sulcus, and left posterior temporal cortex. These results add to our knowledge of the neural basis of semantic control in three ways: (i) Semantic control performance was predicted by the structural covariance network of left pMTG, a site that is less consistently activated than left IFG across studies. (ii) Our results provide further evidence that semantic control is at least partially separable from domain-general executive control. (iii) More flexible patterns of memory retrieval occurred when pMTG co-varied with distant regions in aMFG, as opposed to nearby visual, temporal or parietal lobe regions, providing further evidence that left prefrontal and posterior temporal areas form a distributed network for semantic control.

**Key words:** cortical thickness, resting state, functional connectivity, semantic control, middle temporal gyrus, middle frontal gyrus

## 1. Introduction

Our ability to use semantic knowledge to drive appropriate thoughts and behaviour is fundamental to our mental lives. Semantic cognition is thought to involve at least two interacting components: *conceptual representations* encompass stored knowledge about the meanings of objects, words, sounds and people; while *semantic control* processes shape retrieval to suit our goals and the context (Jefferies 2013; Lambon Ralph et al., 2017). These components are thought to draw on distinct large-scale networks in the brain (Corbett et al., 2011; Davey et al., 2016; Diez et al., 2017; Gold and Buckner, 2002; Gold et al., 2005; Hallam et a., 2018; Humphreys and Lambon Ralph, 2017; Jefferies, 2013; Jefferies and Lambon Ralph, 2006; Patterson et al., 2007; Snowden et al., 2017; Vatansever et al., 2017; Wei et al., 2012). However, little is known about individual differences in these abilities – i.e., what are the structural and functional markers of efficient semantic cognition in healthy participants?

If the capacity to control semantic retrieval is separable from how knowledge is represented, individual differences in task performance should reflect this multi-component structure. Semantic tests will not always measure *what* people know: since concepts have diverse features and associations, the capacity to shape retrieval to suit the circumstances will also have a major impact on performance. Semantic control processes are thought to be required when we have to retrieve non-dominant aspects of knowledge or promote specific aspects of knowledge in the face of strong competition, in order to suit the requirements of the current task or context (Badre et al., 2005; Jefferies, 2013; Lambon Ralph et al., 2017; Thompson-Schill et al., 1997). Semantic control demands are consequently higher when processing the meanings of ambiguous vs. unambiguous words (Rodd et al., 2005; Humphreys and Lambon Ralph, 2017; Whitney et al., 2011), matching items on the basis of a single feature such as colour rather than their global relatedness (Chiou et al., 2018; Davey et al., 2016), retrieving a specific semantic relationship in the face of strong competition, or retrieving weak associations (e.g., SAUCER and ASHTRAY) as opposed to strong associations (e.g., SAUCER and CUP) (Badre and Wagner, 2002; Badre et al., 2005; Davey et al., 2015; Wagner et al., 2001; Whitney et al., 2012). All of these manipulations have in common the need to promote a particular pattern of semantic retrieval which is not typical for that item, and all of these tasks activate a common semantic control network: a meta-analysis of neuroimaging studies including this range of tasks identified a distributed semantic control network that consisted of left inferior frontal gyrus (IFG), posterior middle temporal gyrus (pMTG), dorsal angular gyrus (dAG) bordering intraparietal sulcus (Noonan et al., 2013; see Figure 1). Left IFG is the most

reliably activated site across participants and tasks, while pMTG shows more variation (Vitello et al., 2014), suggesting that pMTG might be especially critical to individual differences in the efficiency of semantic control processes.

Although difficult semantic decisions activate domain-general executive control regions along with other tasks, left pMTG and anterior portions of IFG fall outside the multiple-demand system; they are specifically activated by semantic (or memory) tasks (Humphreys and Lambon Ralph, 2017; Noonan et al., 2013). Left anterior IFG and pMTG show similar functional connectivity in line with the view that they form a network for semantic control (Davey et al., 2016; Humphreys and Lambon Ralph, 2017): interestingly, they show connections with both default mode and multiple-demand regions, which are typically anti-correlated across tasks and resting states (Davey et al., 2016). This distinctive pattern of connectivity might be critical for semantic control, which involves the coordination of brain regions allied to the default mode network that support heteromodal conceptual representations (e.g., Murphy et al., 2018), with control regions that support demanding tasks. By this view, individual differences in semantic control may occur somewhat independently of performance on difficult non-semantic tasks.
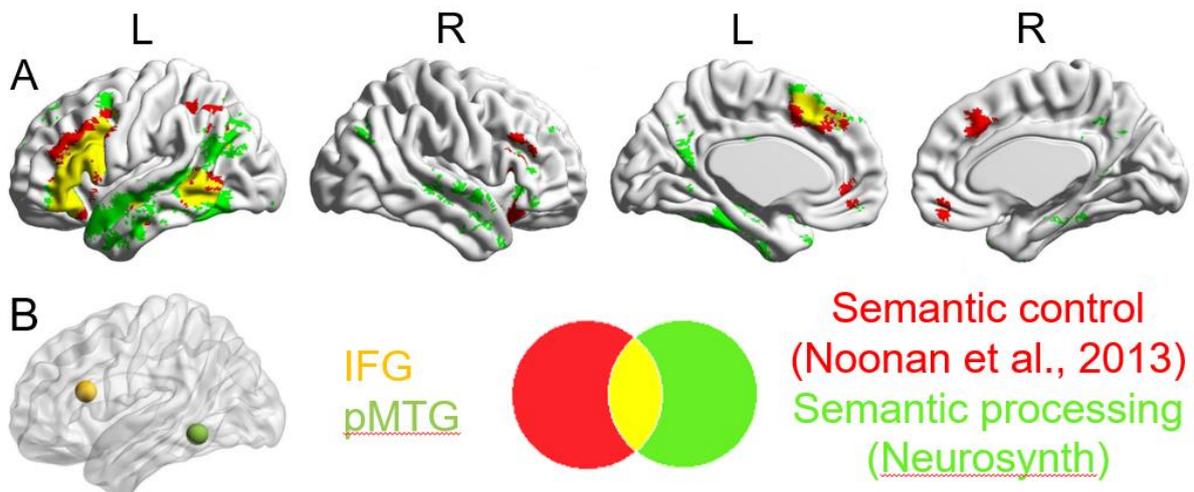


Figure 1. A: Meta-analyses of (i) task contrasts manipulating semantic control demands from Noonan et al. 2013; (in red) and (ii) the term "semantic" from Neurosynth (in green). Semantic regions implicated in control are highlighted in yellow (showing the overlap of the two meta-analyses). B: Seeds for our analysis defined on the basis of these meta-analyses (Noonan et al., 2013). (L= Left hemisphere; R = hemisphere)

A causal role for left IFG and pMTG in semantic control has been established through neuropsychology and brain stimulation. Patients with multimodal semantic deficits in the context of stroke aphasia (i.e. semantic aphasia) have poor control over semantic retrieval, with

largely intact conceptual knowledge, and this pattern is associated with damage to left IFG or temporoparietal regions including pMTG (Hallam et al., 2018; Jefferies and Lambon Ralph, 2006; Noonan et al., 2010; Thompson-Schill et al., 1998). While neuropsychology lacks spatial specificity when drawing inferences about brain-behaviour relationships, inhibitory transcranial magnetic stimulation (TMS) delivered to left IFG and pMTG elicits equivalent disruption of control-demanding semantic judgements: for example, there is an inhibitory effect on the retrieval of weak associations, yet no effect on either strong semantic associations or control-demanding non-semantic decisions (Davey et al., 2015; Hoffman et al., 2010; Whitney et al., 2011). Moreover, damage to left IFG in semantic aphasia and inhibitory TMS to this region in healthy participants elicits an increased response in pMTG to semantic judgements with high control demands (Hallam et al., 2016; 2018), consistent with a pattern of functional compensation within the large-scale distributed semantic control network. The current study supplements these methods by establishing how structural covariation between brain distant regions predicts the efficiency of controlled semantic retrieval across individuals, even after accounting for performance on dominant associations and a non-semantic task.

Although most research in cognitive neuroscience focusses on commonalities across individuals, inter-individual differences can be exploited to understand the neural basis of human cognition (Kanai and Rees, 2011). Cognitive differences between people can be predicted from variation in the structure of specific brain regions (Choi et al., 2008; Schilling et al., 2012). For example, the grey matter density of pre-supplementary motor area (pre-SMA)can account for inter-individual variability in the ability to select the correct response in the presence of response conflict (van Gaal et al., 2011), while the cortical thickness of rostral medial temporal cortex correlates with verbal memory performance (Dickerson et al., 2008). However, cognitive variation is not only associated with the morphometry of individual brain regions but also with structural covariation between regions that form functional networks. For example, people with higher IQ have greater covariation in cortical thickness between IFG and other frontal and parietal brain areas (Lerch et al., 2006). For empathy and theory of mind tasks, structural covariance is more sensitive than regional differences between individuals (Bernhardt et al., 2013; Valk et al., 2017). Consequently, the current study links individual differences in performance on tests of semantic control to structural covariation between posterior temporal and prefrontal regions, as opposed to structural markers for individual sites in pMTG and IFG.

We used cortical thickness measures in around 200 individuals to characterise the structural covariance networks of left IFG and pMTG, two key sites for semantic control in previous group-level neuroimaging analyses (see Figure 1). We examined how these structural covariance networks are modulated by individual differences in the efficiency of semantic control. Specifically, we assessed the identification of weak associations, after controlling for performance on strong associations. This paradigm has been used repeatedly to assess semantic control across different labs and multiple methods (neuroimaging, neuropsychology and TMS): all of these approaches have revealed greater involvement of IFG and pMTG for weak than strong associations (Badre and Wagner, 2002; Badre et al., 2005; Davey et al., 2015; Noppeney et al., 2004; Wagner et al., 2001; Whitney et al., 2011; 2012). When a strong target is not present, control processes are potentially required, both to focus retrieval on the aspects of the probe that relate to the target, and also to select the most relevant potential target from the distractors (Whitney et al., 2011). Consequently, weak association trials are thought to place greater demands on 'controlled retrieval processes' which shape patterns of retrieval away from dominant but currently-irrelevant knowledge and towards weaker yet relevant information (Lorch, 1982). We used a behavioural efficiency metric that combined response time with accuracy, since on this task individuals may trade-off speed and accuracy in different ways. To our knowledge, this is the first cortical thickness investigation of individual differences in semantic control. Previous studies have linked patterns of intrinsic connectivity in semantic regions to individual differences in performance (Mollo et al., 2016; Vatansever et al., 2017; Wei et al., 2012); for example, Wei et al. (2012) found that functional connectivity between left pMTG and other semantic regions, such as IFG and anterior temporal lobe, was positively associated with semantic performance. However, this study did not distinguish between relatively automatic and more controlled aspects of semantic retrieval.

Since brain regions that serve the same functions show greater structural covariance (Lerch et al., 2006), and left IFG and pMTG (amongst other regions) are thought to form a network that supports semantic control (Jefferies and Lambon Ralph, 2006; Jefferies, 2013; Lambon Ralph et al., 2017; Noonan et al., 2013; Whitney et al., 2011), we predicted that seed regions in left IFG and pMTG taken from the meta-analysis of Noonan et al. (2013) would show structural covariance with other regions involved in semantic control. Moreover, since pMTG has more variability than left IFG in the location of activation across individuals (Vitello et al., 2014), we expected that the structural covariance of pMTG with other semantic control regions might be particularly important for predicting individual differences in controlled

semantic retrieval ability. We also hypothesised that the structural covariance of pMTG with other brain areas implicated in semantic control might be more important for performance than the cortical thickness of pMTG alone, since semantic control is supported by a large-scale network and structural covariation between regions forming large-scale functional networks has been shown to be more sensitive to behavioural differences than regional thickness metrics (Bernhardt et al., 2013; Valk et al., 2017). Better performance is often related to greater cortical thickness and great covariation in cortical thickness of task-relevant regions (Alexander-Bloch et al., 2013; Kanai and Rees, 2011; Lerch et al., 2006). Consequently, we anticipated participants with high performance on weak associations would show stronger structural covariance between left pMTG and other semantic control regions.

## 2. Method

### 2.1 Participants:

The research was approved by the York Neuroimaging Centre and Department of Psychology ethics committees. We recruited 207 healthy adults from the University of York (137 females; age: mean ± SD = 20.21 ± 2.35, range: 18 – 31 years). This sample included the 154 participants studied by Vatansever et al. (2017) and Sormaz et al. (2017). All participants were right handed, native English speakers, with normal or corrected-to-normal vision and no history of psychiatric or neurological illness. All volunteers provided written informed consent, were paid or given course credit for their participation and were debriefed after the study was completed. We removed from the analysis fifteen participants with missing behavioural data; two without neuroimaging data; ten without appropriate cortical thickness pre-processing and two because accuracy was not higher than chance in at least one of the tasks.

### 2.2 Procedure:

An initial MRI session included a structural scan and a 9-minute resting-state sequence. Within a week of the scan, participants completed a large battery of computer-based tasks in three behavioural testing sessions, each lasting two hours. These measures included weak and strong semantic associations and a non-semantic control task with similar perceptual and motor requirements. The contrast between strong and weak associations was selected from the task battery because it closely maps onto manipulations of semantic control used in previous task-based fMRI studies, and because the stimuli presented in these conditions were matched for

psycholinguistic properties (see below). The order of these tasks and the order of sessions was counterbalanced across participants. For a more complete description of those aspects of cognitive testing that fall outside the scope of the current study, see Vatansever et al. (2017).

2.3 Tasks:

The tasks employed a three-alternative force choice design. A probe was presented with a target and two unrelated distracters, which were targets in other trials. Each trial started with a blank screen for 500ms. The response options were subsequently presented at the bottom of the screen for 900ms. Finally, the probe was presented at the top of the screen, triggering the onset of the decision-making period. The probe and choices remained visible until the participant responded, or for a maximum of 3 seconds. Both response time (RT) and accuracy were recorded. See Figure 2 for an example trial for each task.

2.3.1 Weak and strong association matching: Participants were asked to select the target word that was most strongly associated with a probe picture. The semantic association that linked probes and targets was either strong (BRASS INSTRUMENT – ORCHESTRA) or weak (BRASS INSTRUMENT – PARADE). For strongly-linked items, semantic control demands are thought to be minimised because task-relevant information is relatively easy to retrieve. In contrast, controlled retrieval processes are thought to be required to identify weakly-associated targets, since task-relevant aspects of knowledge are not the most strongly-encoded aspects of knowledge; therefore, semantic activation may need to be 'shaped' to focus on the specific aspects of knowledge that are relevant to the association being probed. This manipulation has been used in many previous task-based fMRI studies (Badre et al., 2005; Davey et al., 2016; Noppeney et al., 2004; Wagner et al., 2001) and TMS studies (Davey et al., 2015; Whitney et al., 2011) of semantic control, highlighting a role for pMTG alongside IFG in controlled semantic retrieval. The strong and weak trials were selected from a large database used in previous experiments (Krieger-Redwood, 2012; Davey et al., 2015). The strength of association between probe-target pairs was assessed using a 7-point Likert scale, along with the familiarity and imageability for each member of the pair. The mean association rating between probes and targets was 6.02 for 'strong' pairs and 3.32 for 'weak' pairs ($t(118) = 21.74$; $p < 0.001$). There were no differences between conditions in word length, familiarity, imageability or lexical frequency (Table 1). There were sixty strong and

sixty weak association trials, presented in four blocks of thirty trials each. The order of trials within each block was randomized across subjects.

2.3.2 Figure matching task: This was a non-semantic control task, with similar perceptual and decision-making demands to the semantic judgments. The stimuli were sixty pixelated and scrambled black-and-white photographs of faces (taken from Krieger-Redwood, 2012). Participants were asked to select the target that was identical to the probe; the distracters were the same images rotated by 180° or 270°. The task was split in two blocks of thirty trials each.
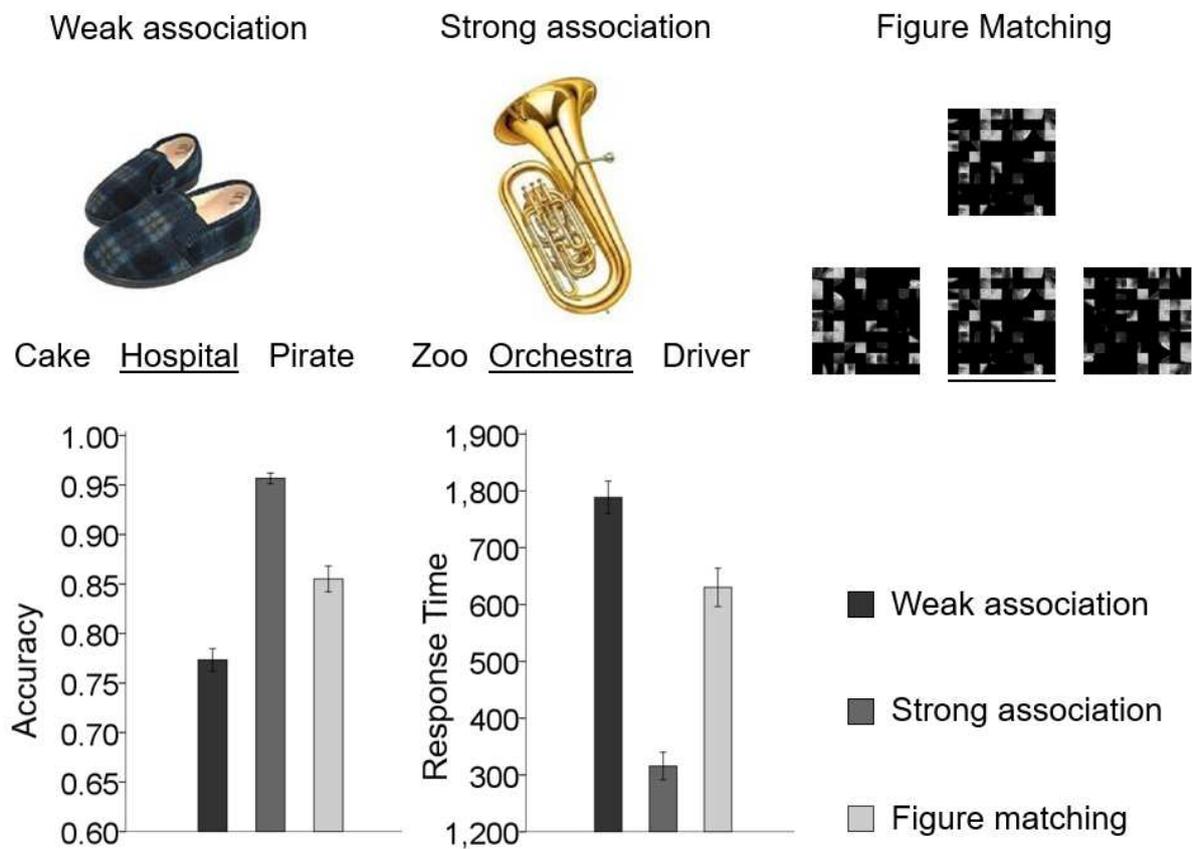


Figure 2. Top row: Illustration of the behavioural tasks. For all the tasks, correct answers are underlined. Bottom row: Mean accuracy and response time for each task. Error bars represent 95% confidence intervals.

Table 1 Psycholinguistic variables for weakly and strongly-associated target words.

| Target | | Mean | SD | t | Sig. |
|---|---|---|---|---|---|
| Word length | Strong association | 6.43 | 0.39 | -0.16 | 0.873 |
| | Weak association | 6.6 | 0.34 | | |
| Lexical Frequency | Strong association | 13564.8 | 1887 | 0.89 | 0.374 |
| | Weak association | 11233.6 | 1805 | | |
| Familiarity | Strong association | 6.02 | 0.09 | -0.88 | 0.381 |
| | Weak association | 6.12 | 0.08 | | |
| Imageability | Strong association | 5.16 | 0.13 | 1.07 | 0.287 |
| | Weak association | 4.96 | 0.13 | | |
| Semantic association | Strong association | 6.02 | 0.07 | 21.74 | 0.000 |
| | Weak association | 3.32 | 0.10 | | |

## 2.4 MRI data acquisition:

MRI data was acquired using a 3T GE HDx Excite Magnetic Resonance Imaging (MRI) system utilising an eight-channel phased array head coil tuned to 127.4 MHz, at the York Neuroimaging Centre, University of York. Structural MRI acquisition in all participants was based on a T1-weighted 3D fast spoiled gradient echo sequence (TR = 7.8 s, TE = minimum full, flip angle = 20°, matrix size = 256 × 256, 176 slices, voxel size = 1.13 × 1.13 × 1 mm). A nine-minute resting state fMRI scan was carried out using single-shot 2D gradient-echo-planar imaging (TR = 3s, TE = minimum full, flip angle = 90°, matrix size = 64 × 64, 60 slices, voxel size = 3 × 3 × 3 mm$^3$, 180 volumes). Participants were asked to passively view a fixation cross and not to think of anything in particular during the resting-state scan. A FLAIR scan with the same orientation as the functional scans was collected to improve co-registration between subject-specific structural and functional scans.

## 2.5 Data pre-processing:

2.5.1 Behavioural data: To account for potential speed-accuracy trade-offs, inverse efficiency scores were used as the dependent measure: i.e., the mean RT for correct responses in each task was divided by the proportion of correct responses (Townsend and Ashby, 1983). We reversed this measure so that higher efficiency scores would correspond to better performance. Inverse efficiency is commonly used to measure behaviour performance (Wei et

al., 2012), because it accounts for differences between individuals in the way that accuracy and speed are traded-off against each other. Outlying values (±3SD) were replaced with mean ±3SD. Finally, we calculated z-scores for each task across subjects before performing any analyses.

2.5.2 Cortical thickness measurements: FreeSurfer was used to estimate vertex-wise cortical thickness (5.3.0; https://surfer.nmr.mgh.harvard.edu), using an automated surface reconstruction scheme described in detail elsewhere (Dale et al., 1999; Fischl et al., 1999; Fischl and Dale 2000; Fischl et al. 2001). Briefly, the following processing steps were applied: intensity normalization, removal of non-brain tissue, tissue classification and surface extraction. Cortical surfaces were visually inspected and corrected if necessary. Cortical thickness was calculated as the closest distance between the grey/white matter boundary and pial surface at each vertex across the entire cortex. A surface-based smoothing with a full-width at half maximum (FWHM) = 20mm was applied. Surface alignment based on curvature to an average spherical representation, fsaverage5, was used to improve correspondence of measurement locations among subjects.

2.5.3 Resting state pre-processing: All pre-processing of resting-state data was achieved using FMRIB Software Library (FSL version 4.0, http://fsl.fmrib.ox.ac.uk/fsl/fslwiki/FEAT/). The Brain Extraction Tool (BET) was used to extract individual FLAIR and T1 weighted structural brain images. Structural images were linearly registered to the MNI-152 template using FMRIB's Linear Image Registration Tool (FLIRT). FMRI Expert Analysis Tool (FEAT) was used to perform the following standard analysis steps: (1) correcting for head movement using MCFLIRT; (2) slice timing correction using Fourier space time-series phase-shifting; (3) spatial smoothing with 6mm full-width half-maximum (FWHM) Gaussian kernel; (4) grand mean intensity normalisation of the entire 4D dataset by a single multiplicative factor; (5) high pass (sigma = 100s) and low pass (sigma = 2.8s) temporal filtering (Gaussian-weighted least-squares straight line fitting). In each analysis, eleven nuisance regressors were removed, including the confounding six head motion parameters and the top five principal components extracted from white matter (WM) and cerebrospinal fluid (CSF) masks using the CompCor method (Behzadi et al., 2007). We did not perform global signal regression which was reported to introduce spurious anti-correlations (Murphy et al., 2009). We generated WM and CSF masks from each individual's structural image (Zhang et al., 2001).

<u>2.6 Data analysis:</u>

2.6.1 Cortical thickness analysis: The SurfStat toolbox for Matlab [http://www.math.mcgill.ca/keith/surfstat/] (Worsley et al., 2009) was used for structural covariance network analysis, as in previous studies (Bernhardt et al., 2013; Valk et al., 2017). Two seeds, left IFG (MNI -47 21 18) and left pMTG (MNI -58 -49 -9), were taken from an fMRI meta-analysis of semantic control (Noonan et al., 2013) (Figure 1). These sites were the regions with the highest t-values in the meta-analysis of semantic control studies (Noonan et al., 2013) and the most reliably implicated in semantic control across participants in previous fMRI and neuropsychological studies. We placed a sphere (radius = 3mm) around each peak to create the regions of interest (ROIs). To find regions that strongly co-varied with left IFG or left pMTG in cortical thickness, we constructed a structural covariance network for each seed by correlating the thickness of each seed with thickness measures across all cortical surface points. There is a well-established negative correlation between age and cortical thickness (Tamnes et al., 2010) and gender also influences cortical thickness (Luders et al., 2006); consequently, these variables were included as covariates of no interest. The model fitted at surface point *i* was:

$$T_i = \beta 0 + \beta 1 * Sex + \beta 2 * Age + \beta 3 * T_{seed}$$

where $T_{seed}$ is the seed thickness. We determined significant clusters in this model using random field theory for nonisotropic images (Worsley et al., 1999) which controlled the Family-Wise Error rate at $p < 0.05$. We also applied Bonferroni correction to account for the fact that we included two models (IFG and pMTG); consequently, the final threshold set by FWE correction was $p < 0.025$.

To assess the relationship between structural covariance strength and individual differences in controlled semantic retrieval, we added performance on strong and weak associations, plus the interaction between performance on weak association trials and cortical thickness of the seed, to the model above. Therefore, the final model was:

$$T_i = \beta 0 + \beta 1 * Sex + \beta 2 * Age + \beta 3 * T_{seed} + \beta 4 * Strong\ associations + \beta 5 * Weak\ associations + \beta 6 * (T_{seed} * Weak\ associations)$$

where $T_{seed} *$ Weak associations denotes an interaction. A positive interaction indicates stronger structural correlation with better performance on weak associations, while a negative interaction indicates weaker structural covariation for better performance. To assess the

specificity of this effect to semantic processing, we performed a control analysis that included the non-semantic figure matching task as an additional covariate, using the following model:

$T_i = \beta0 + \beta1 * Sex + \beta2 * Age + \beta3 * T_{seed} + \beta4 * Strong\ associations + \beta5 * Weak\ associations + \beta6 * Figure\ matching + \beta7 * (T_{seed} * Weak\ associations)$.

Moreover, since weak associations are more difficult to retrieve than strong associations, we investigated whether similar results would emerge from the comparison of a more difficult non-semantic task with an easier semantic task, using the following model:

$T_i = \beta0 + \beta1 * Sex + \beta2 * Age + \beta3 * T_{seed} + \beta4 * Strong\ associations + \beta5 * Figure\ matching + \beta6 * (T_{seed} * Figure\ matching)$

where $T_{seed} * Figure\ matching$ denotes an interaction.

Finally, while most of our analysis focused on structural covariance between purported semantic control regions, reflecting the accepted view that cognitive abilities reflect the coordinated action of multiple brain regions, we also examined the relationship between task performance and cortical thickness within each of our ROIs (left IFG and pMTG). In these analyses, we examined partial correlations between cortical thickness in a specific region and performance on specific pair of tasks (e.g., weak associations controlling for strong associations).

2.6.2 Resting state functional connectivity analysis: Regions found in structural covariance analysis and corresponding seeds were subsequently used to define ROIs in an analysis of intrinsic connectivity, measured using fMRI at rest. We identified the peak vertex in each cluster in the cortical thickness analysis, obtained the coordinates of that vertex in MNI305 space and transformed to MNI152 space. We placed a sphere (radius = 3mm) around this peak. The time series from each ROI was extracted and used as an explanatory variable in the first-level connectivity analysis. In the high-level analysis, the averaged functional connectivity map derived from each ROI was generated. Finally, we conducted a conjunction analysis, exploring the regions that showed stronger functional connectivity with both regions via a formal conjunction analysis, using FSL's 'easythresh_conj' tool (Nichols et al., 2005). For all contrasts, age, gender and head movement parameters were included as covariates of no interest. To control for multiple comparisons, we considered the number of voxels in the

brain and used a cluster forming threshold of Z > 3.1 (P < 0.05). Brain networks were visualized using BrainNet Viewer (Xia et al., 2013).

## 3. Results

### 3.1 Behavioural results:

Figure 2 shows mean accuracy and RT for each task. As expected, weak association matching was more difficult than strong association matching (inverse efficiency: t = 41.787, p < 0.001). Inverse efficiency for the non-semantic control task, involving meaningless figure matching, fell between strong and weak association trials (figure matching vs. weak associations: t = -12.023, p <0.001; figure matching vs. strong associations: t = 20.237, p <0.001).

### 3.2 Structural covariance network:

To find regions that co-vary strongly with IFG and pMTG, we constructed the structural covariance networks of these two regions. The seed in left IFG was correlated with bilateral IFG and inferior frontal sulcus, right middle frontal gyrus and right middle cingulate cortex (FWE, p < 0.025; Figure 3A). Patterns of structural correlations from the seed in left pMTG encompassed regions in left anterior superior temporal gyrus, left inferior parietal sulcus and right lateral occipital cortex (FWE, p < 0.025; Figure 3B). Together, these patterns of structural covariance encompassed or lay adjacent to many of the key regions implicated in semantic control (i.e., by the meta-analysis of Noonan et al., 2013). Moreover, the sites within intraparietal sulcus and mid-cingulate cortex were distant from both seeds.
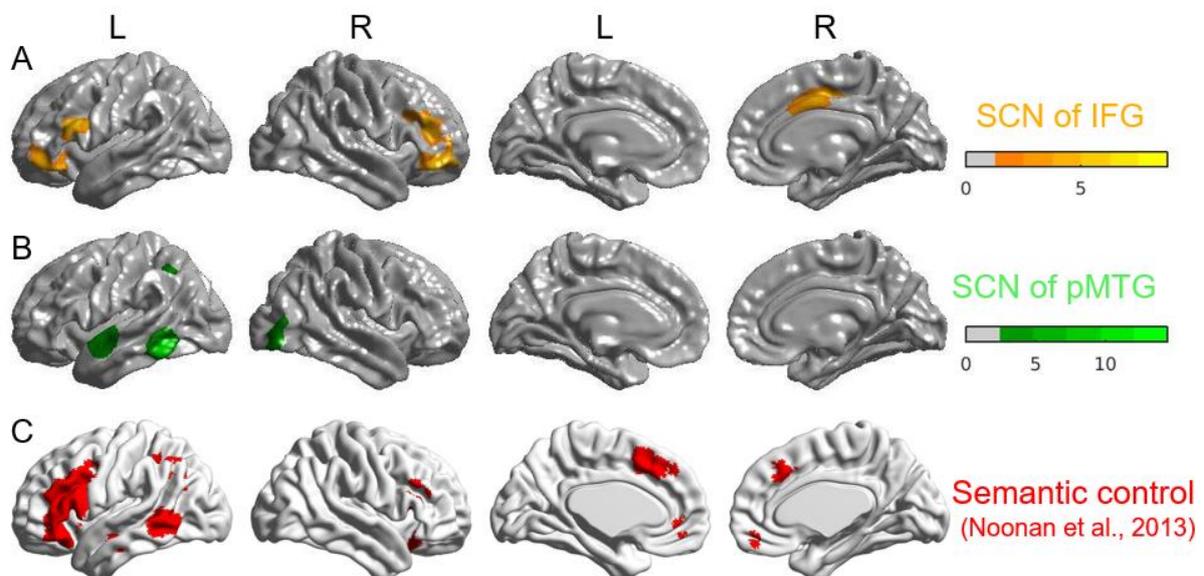
Figure 3. Structural covariance analysis seeding from (A) left IFG and (B) left pMTG (FWE-corrected, p<0.025). C: The meta-analysis of semantic control network (red colour) (Noonan et al., 2013). (L= Left hemisphere; R = Right hemisphere)

### 3.3 Relationship between structural covariance and controlled semantic retrieval:

To assess the relationship between structural covariance networks and the efficiency of controlled semantic retrieval, we investigated the parametric interaction between seed covariance strength and inter-individual differences in performance on weak association trials, controlling for performance on strong associations. The structural covariance network of left IFG was not modulated by weak associations (FWE, p<0.025). However, structural correlations from left pMTG to left anterior middle frontal gyrus (aMFG) were positively modulated by weak associations (FWE, p<0.025) (Figure 4). In other words, individuals with higher weak association performance showed stronger structural covariance between left pMTG and left aMFG relative to those with lower performance. To further characterise this interaction, we subdivided the group according to performance on weak association trials (above and below median). Individuals who showed good retrieval of weak associations showed a positive correlation between the cortical thickness of left aMFG and pMTG. For participants who were poorer at retrieving weak associations, there was no correlation (Figure 4).
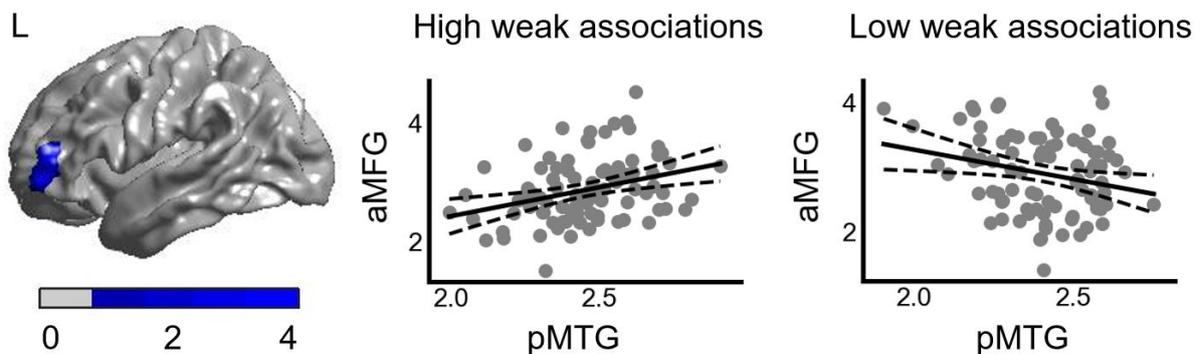


Figure 4. Interaction between the degree of structural covariance of left pMTG and weak associations after controlling for age, gender and strong associations (FWE-corrected, p<0.025). To illustrate the parametric interaction effect, regression fits are shown after the group has been split into two groups according to median performance on weak associations. (L= Left hemisphere.)

A series of supplementary analyses assessed the robustness and specificity of this effect. Identical results were obtained when figure matching was added as an additional covariate: the structural covariance between pMTG and aMFG still predicted weak associations after controlling for both strong associations and figure matching (FWE, p < 0.025). To establish if

the same pattern of structural covariance between pMTG and aMFG would be observed for more difficult decisions in general, or whether the effect is specific to semantic control, we also contrasted the non-semantic figure matching task with the easier strong association judgements. This analysis did not highlight structural covariation between pMTG and aMFG. Instead, pMTG co-varied with a region of dorsal anterior cingulate/pre-SMA to a greater extent in people who were more efficient at making perceptual decisions in the figure matching task (FWE, $p < 0.05$, Figure 5). This effect did not survive Bonferroni correlation for the number of seeds used in the analysis, although it was robust to FWE correction for multiple comparisons and therefore it is included here for completeness.
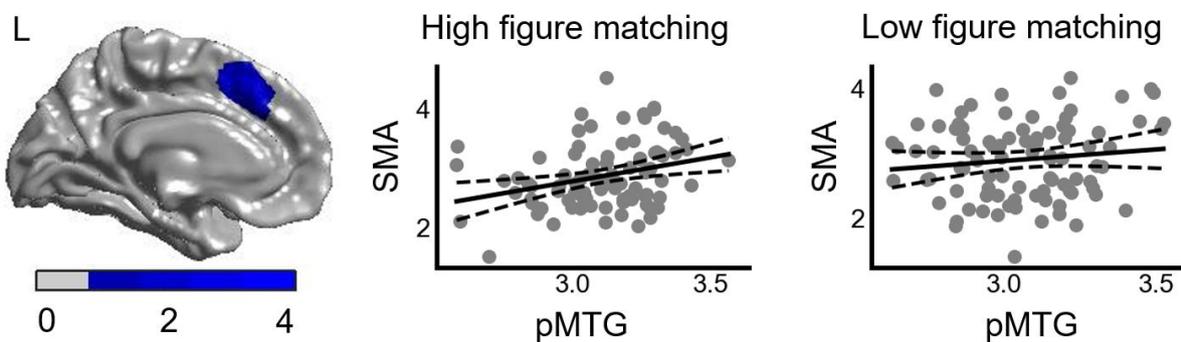


Figure 5. Interaction between the degree of structural covariance of left pMTG seed region and figure matching after controlling for age, gender and strong associations (FWE-corrected, $p<0.05$) To illustrate the parametric interaction effect, regression fits are shown after the group was split into two groups according to the median of performance on figure matching. (L = left hemisphere.)

3.4 ROI-based cortical thickness analysis:

We conducted ROI-based cortical thickness to examine the relationship between cortical thickness in pMTG and IFG individually and semantic control performance. These regions were defined by a meta-analysis of task-based fMRI studies of semantic control (Noonan et al., 2013). The cortical thickness of left pMTG correlated with weak associations ($r = 0.186$, $p = 0.013$), but this effect only approached significance after controlling for performance on strong associations ($r = 0.135$, $p = 0.075$). There was no correlation between cortical thickness of left IFG and weak associations ($r = 0.107$, $p = 0.157$). This suggests that the structural covariation of pMTG with aMFG predicts the efficiency of controlled semantic retrieval more successfully than the cortical thickness of individual regions previously implicated in this function.

3.5 Resting-state functional connectivity:

Given the evidence above that structural covariance between left pMTG and aMFG predicts the efficient retrieval of weak associations, we examined the intrinsic functional connectivity of these two sites using resting-state fMRI. The peak from the cortical thickness analysis in left aMFG (MNI coordinates: -40, 47, 9) and the pMTG peak from Noonan et al.'s (2013) meta-analysis (MNI coordinates: -58 -49 -9) were used as seeds. We found substantial overlap between the patterns of intrinsic connectivity for these sites. They both showed correlations through time with extensive regions of left prefrontal cortex, including inferior frontal sulcus, plus anterior and dorsolateral aspects of prefrontal cortex, similar but less extensive prefrontal regions in the right hemisphere, posterior middle and inferior temporal cortex, dorsal angular gyrus bordering intraparietal sulcus and pre-SMA. We computed a formal conjunction of these patterns of functional connectivity. This showed striking similarity with the semantic control network established from a meta-analysis of task-based fMRI studies (Figure 6).
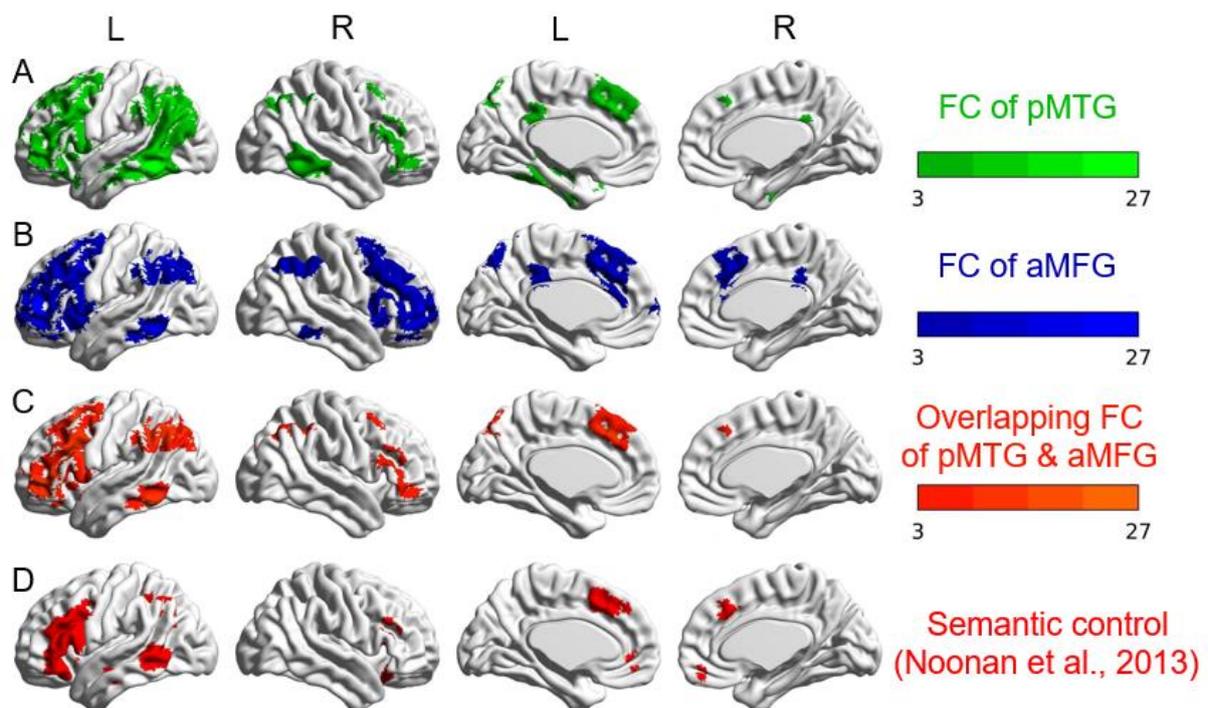


Figure 6. The positive functional connectivity (FC) networks from (A) pMTG and (B) aMFG (FWE-corrected, p<0.025). A direct comparison between (C) the conjunction of functional connectivity for pMTG and anterior MFG and (D) a meta-analysis of semantic control (Noonan et al., 2013). (L = Left hemisphere; R = Right hemisphere.)

<u>4. Discussion</u>

This study investigated the biological basis of individual differences in semantic control using cortical thickness metrics in a large sample of around 200 participants. We found that a key semantic control region from the task activation literature, left pMTG, showed stronger structural covariation with aMFG in people who showed relatively efficient controlled semantic retrieval. A similar network including posterior temporal and anterior and inferior prefrontal regions shows activation during fMRI studies of control-demanding semantic tasks. This pattern of structural covariation was observed even when we controlled for performance on similar non-semantic decisions. Moreover, the structural covariance between pMTG and aMFG did not predict performance when a relatively demanding non-semantic figure matching task was contrasted with easier judgements of strong semantic associations, suggesting the effect was specific to control-demanding patterns of semantic retrieval. The two sites showing structural covariation also had highly overlapping patterns of intrinsic connectivity at rest, consistent with the view that these regions form a functional network. This intrinsic connectivity network resembled the set of distributed brain regions that show stronger activation when semantic control demands are high (Noonan et al., 2013). The overlapping intrinsic connectivity for pMTG and aMFG included domain-general executive control regions, such as inferior frontal sulcus and pre-SMA, as well as sites within the default mode network, in left angular gyrus and dorsolateral prefrontal cortex, in line with the findings of Davey et al. (2016) who proposed that semantic control regions show strong connectivity at rest to these two networks that are normally anti-correlated.

The suggestion that pMTG contributes to semantic control remains controversial since temporal lobe regions are not traditionally thought to contribute to the executive control of behaviour. However, a meta-analysis of task-based fMRI studies identified pMTG as the second most reliably activated region across diverse manipulations of semantic control, after left IFG (Noonan et al., 2013) and numerous individual studies have reported responses in both left IFG and pMTG for the contrast of weak over strong associations (Davey et al., 2016; Gold et al., 2006). The interpretation of these effects has remained unclear since greater activation in pMTG could arguably reflect increased activation of conceptual knowledge in more demanding tasks. Studies have shown that inhibitory stimulation of pMTG disrupts the retrieval of weak associations more than strong associations (Davey et al., 2015; Whitney et al., 2011), suggesting that this region does play a critical role. However, the potential for individual differences analyses to inform our understanding of brain-behaviour relationships is under-

exploited. The current results therefore make an important contribution to knowledge by showing that if pMTG co-varies in cortical thickness with a region in aMFG, participants tend to be more efficient at retrieving weak associations. These observations are also consistent with a previous study which found that pMTG activation to control-demanding semantic tasks is more variable in location and intensity across participants than the response in left IFG (Vitello et al., 2014). This finding might reflect differences between people in the extent to which pMTG is recruited to support semantic control – i.e., people might universally recruit left IFG but those people who also recruit pMTG might show the most efficient controlled semantic retrieval, and also the strongest structural covariation between pMTG and left aMFG.

Interestingly, the pattern of structural covariation between sites appeared to be a better predictor of performance on semantic control tests than the overall thickness of left pMTG itself, in line with a network view of cognitive functions. Previous studies have found that structural markers of social cognitive ability are also reflected in interregional networks as opposed to anatomical variation within specific regions. For example, the structural covariance network of dorsal anterior insula, but not its thickness, correlated with individual differences in empathic responding (Bernhardt et al., 2013) and structural covariance analysis, not regional thickness mapping, found a double dissociation between empathy and mentalizing (Valk et al., 2017). Structural covariance might reflect persistent cross-talk between regions: brain regions that show stronger correlation in cortical thickness are often part of systems that are known to sub-serve particular cognitive functions (Alexander-Bloch et al., 2013; Evans 2013). For example, individuals with greater cortical thickness in posterior parts of inferior frontal cortex (Broca's area) typically also have greater cortical thickness in superior temporal cortex (Wernicke's area) (Lerch et al., 2006). We also observed similarities between structural covariance patterns and measures of intrinsic connectivity. The functional connectivity of the regions forming a structural covariance network, i.e., pMTG and aMFG, had similar patterns of functional connectivity at rest. Previous studies have also found that patterns of intrinsic functional connectivity show striking overlap with grey matter co-variance (Seeley et al., 2009; Segall, et al., 2012) and give rise to similar network parcellations (Kelly et al., 2012). These findings are consistent with the view that structural covariance might relate to greater cross-talk between regions.

Our results are also consistent with a functional dissociation between semantic and domain-general executive control; however, this is not solely based on the role of specific sites, but instead on their participation in distinct large-scale networks. We found that structural

covariance between left pMTG and left aMFG predicted performance on weak associations even after controlling for strong associations (a task comparison that is thought to highlight controlled semantic retrieval; cf. Badre et al, 2005; Whitney et al., 2011). However, this pattern did not predict performance on a relatively demanding non-semantic task. These findings are consistent with the proposal that interactions between pMTG and anterior parts of prefrontal cortex support relatively abstract or internally-directed aspects of control – i.e., processes that establish which representations to prioritise when an association between two items is weak, as opposed to supporting the capacity to select a relevant response across tasks more generally (Badre and Wagner, 2007; Tomita et al., 1999). In a similar way, both left pMTG and anterior aspects of IFG show stronger activation for difficult semantic tasks but not executively-demanding non-semantic tasks (Humphreys and Lambon Ralph, 2017) and inhibitory TMS to both sites disrupts the retrieval of weak associations, yet has no effect on harder perceptual judgements (Whitney et al., 2011). Both pMTG and anterior parts of inferior and middle frontal cortex lie outside the multiple-demand system implicated in cognitive control across domains (Duncan, 2010; Fedorenko et al., 2013), although they are involved in controlled retrieval from memory (Barredo et al., 2015; Humphreys and Lambon Ralph, 2017; Noonan et al., 2013; Whitney et al., 2011).

In contrast, structural covariation between pMTG and pre-SMA predicted performance on a relatively demanding non-semantic task, relative to an easier semantic task probing strong associations. This result suggests that pMTG is not exclusively a semantic control region, but rather can participate in multiple large-scale functional networks – individual differences in structural covariation might reflect which of these networks is dominant in an individual. At the group level, pMTG structurally co-varied with both domain-general control and visual regions, as well as with cortical regions implicated in semantic processing. In line with this observation, previous work has shown that pMTG functionally couples to many different networks at rest (Braga et al., 2013). This diverse pattern of connectivity could be crucial to explaining the varied links between structural covariance of pMTG and behaviour in the current study. When pMTG co-varies with left prefrontal regions (implicated in memory control), the capacity for controlled semantic retrieval is high. In contrast, the pre-SMA region showing covariation with pMTG in people who did well at the non-semantic task is implicated in domain-general executive control (Duncan, 2010; Duncan and Owen, 2000; Fedorenko et al., 2013; Thompson and Duncan, 2009). In the meta-analysis of Noonan et al. (2013), pre-SMA showed a stronger response to control-demanding semantic tasks, but this cluster was also

implicated in phonological control. In line with the suggestion that pre-SMA contributes to the multiple-demand system, it shows stronger activation for difficult vs. easy task conditions across domains, including spatial working memory, verbal working memory, maths and music (Fedorenko et al., 2013). Inhibitory TMS to pre-SMA induces deficits related to task switching (Rushworth et al., 2002), conflict resolution (Mars et al, 2009), response inhibition (Chen et al., 2009) and complex movement sequencing (Lau et al., 2007). Consequently, although pre-SMA contributes to lexical-semantic tasks (Chee et al., 1999; Moore-Parks et al., 2010; Ulrich et al., 2013), its functional role is not constrained to this domain; instead it is thought to contribute to aspects of cognitive control such response selection and switching (Hertrich et al., 2016). Our data are consistent with this domain-general role for pre-SMA, although this network-based dissociation requires replication since the pre-SMA cluster did not survive Bonferroni correction for the number of seeds in our analysis.

Left pMTG shows a pattern of intrinsic connectivity that overlaps with the frontoparietal network (Yeo et al., 2011) (see Figure 6). Our finding that pMTG forms structural covariance networks with distinct sites, with diverse consequences for task performance, is consistent with studies showing that this network implements a wide range of task demands by rapidly updating its functional connectivity to suit the circumstances (Cole et al., 2013; Dixon et al., 2018). The frontoparietal network shows stronger shifts in brain-wide functional connectivity patterns across task states than other networks, and these connectivity patterns can be used to identify the current task (Cole et al., 2013). pMTG in particular shows diverse patterns of functional connectivity when compared with other frontoparietal sites (Dixon et al., 2018). These recent observations might relate directly to our findings that pMTG covariation with anterior PFC supports semantic control, while covariation with pre-SMA supports task performance on demanding non-semantic judgements.

One limitation of our study is that we examined structural covariation from specific seeds in the left hemisphere associated with semantic control. We cannot exclude the possibility that other sites might be relevant for performance on our tasks. In particular, our task had some similarities (although also some important differences) with tests of divergent thinking, such as the remote associates task, which require participants to identify shared distant associations across multiple items (Bendetowicz et al., 2017; Chermahini et al., 2012; Mednick, 1962; Mednick et al., 1964). Although the semantic control literature, including studies employing contrasts of weak and strong associations to single items, have identified a clear role for the left-lateralised semantic control system (as in this experiment; see Noonan et

al., 2013 and Lambon Ralph et al., 2017 for a review), the creativity literature has emphasised a possible role for the right hemisphere in "coarse coding" – i.e., the representation or retrieval of peripheral meanings and features (Jung-Beeman, 2005; Tompkins et al., 2008). For example, the generation of unusual associations co-activated the right medial prefrontal regions (Green et al., 2015) and damage to this region affected the ability to generate remote ideas (Bendetowicz et al., 2017). In future work, the potential contribution of right-lateralised regions to semantic control should be examined.

## 5. Conclusions

In summary, our study documented structural networks that predicted the capacity of individuals to perform well on tests tapping controlled semantic retrieval. The cortical thickness of left pMTG and anterior prefrontal cortex together predicted the capacity to retrieve weak associations. Functionally-significant individual differences in structure were reflected in interregional networks rather than in the anatomy of specific regions.

## References

Alexander-Bloch, A., Raznahan, A., Bullmore, E., Giedd, J., 2013. The convergence of maturational change and structural covariance in human cortical networks. Journal of Neuroscience 33, 2889-2899.

Badre, D., Poldrack, R.A., Pare-Blagoev, E.J., Insler, R.Z., Wagner, A.D., 2005. Dissociable controlled retrieval and generalized selection mechanisms in ventrolateral prefrontal cortex. Neuron 47, 907-918.

Badre, D., Wagner, A.D., 2007. Left ventrolateral prefrontal cortex and the cognitive control of memory. Neuropsychologia 45, 2883-2901.

Badre, D., & Wagner, A. D. (2002). Semantic retrieval, mnemonic control, and prefrontal cortex. Behavioral and cognitive neuroscience reviews, 1(3), 206-218.

Barredo, J., Oztekin, I., Badre, D., 2015. Ventral Fronto-Temporal Pathway Supporting Cognitive Control of Episodic Memory Retrieval. Cerebral Cortex 25, 1004-1019.

Behzadi, Y., Restom, K., Liau, J., Liu, T.T., 2007. A component based noise correction method (CompCor) for BOLD and perfusion based fMRI. Neuroimage 37, 90-101.

Bendetowicz, D., Urbanski, M., Aichelburg, C., Levy, R., Volle, E., 2017. Brain morphometry predicts individual creative potential and the ability to combine remote ideas. Cortex 86, 216-229.

Bernhardt, B.C., Klimecki, O.M., Leiberg, S., Singer, T., 2013. Structural covariance networks of the dorsal anterior insula predict females' individual differences in empathic responding. Cerebral Cortex 24, 2189-2198.

Braga, R.M., Sharp, D.J., Leeson, C., Wise, R.J., Leech, R., 2013. Echoes of the brain within default mode, association, and heteromodal cortices. Journal of Neuroscience 33, 14031-14039.

Chee, M.W., O'Craven, K.M., Bergida, R., Rosen, B.R., Savoy, R.L., 1999. Auditory and visual word processing studied with fMRI. Human brain mapping 7, 15-28.

Chen, C.-Y., Muggleton, N.G., Tzeng, O.J., Hung, D.L., Juan, C.-H., 2009. Control of prepotent responses by the superior medial frontal cortex. Neuroimage 44, 537-545.

Chermahini, S.A., Hickendorff, M., Hommel, B., 2012. Development and validity of a Dutch version of the Remote Associates Task: An item-response theory approach. Thinking Skills and Creativity 7, 177-186.

Chiou, R., Humphreys, G.F., Jung, J., Ralph, M.A.L., 2018. Controlled semantic cognition relies upon dynamic and flexible interactions between the executive 'semantic control'and hub-and-spoke 'semantic representation' systems. Cortex 103, 100 -116.

Choi, Y.Y., Shamosh, N.A., Cho, S.H., DeYoung, C.G., Lee, M.J., Lee, J.-M., Kim, S.I., Cho, Z.-H., Kim, K., Gray, J.R., 2008. Multiple bases of human intelligence revealed by cortical thickness and neural activation. Journal of Neuroscience 28, 10323-10329.

Cole, M.W., Reynolds, J.R., Power, J.D., Repovs, G., Anticevic, A., Braver, T.S., 2013. Multi-task connectivity reveals flexible hubs for adaptive task control. Nature Neuroscience 16, 1348.

Corbett, F., Jefferies, E., Lambon Ralph, M.A., 2011. Deregulated semantic cognition follows prefrontal and temporo-parietal damage: evidence from the impact of task constraint on nonverbal object use. Journal of Cognitive Neuroscience 23, 1125-1135.

Dale, A.M., Fischl, B., Sereno, M.I., 1999. Cortical surface-based analysis: I. Segmentation and surface reconstruction. Neuroimage 9, 179-194.

Davey, J., Cornelissen, P.L., Thompson, H.E., Sonkusare, S., Hallam, G., Smallwood, J., Jefferies, E., 2015. Automatic and Controlled Semantic Retrieval: TMS Reveals Distinct Contributions of Posterior Middle Temporal Gyrus and Angular Gyrus. Journal of Neuroscience 35, 15230-15239.

Davey, J., Thompson, H.E., Hallam, G., Karapanagiotidis, T., Murphy, C., De Caso, I., Krieger-Redwood, K., Bernhardt, B.C., Smallwood, J., Jefferies, E., 2016. Exploring the role of the posterior middle temporal gyrus in semantic cognition: Integration of anterior temporal lobe with executive processes. Neuroimage 137, 165-177.

Dickerson, B.C., Fenstermacher, E., Salat, D.H., Wolk, D.A., Maguire, R.P., Desikan, R., Pacheco, J., Quinn, B.T., Van der Kouwe, A., Greve, D.N., 2008. Detection of cortical thickness correlates of cognitive performance: reliability across MRI scan sessions, scanners, and field strengths. Neuroimage 39, 10-18.

Díez, E., Gómez-Ariza, C.J., Diez-Alamo, A.M., Alonso, M.A., Fernandez, A., 2017. The processing of semantic relatedness in the brain: Evidence from associative and categorical false recognition effects following transcranial direct current stimulation of the left anterior temporal lobe. Cortex 93, 133-145.

Dixon, M.L., De La Vega, A., Mills, C., Andrews-Hanna, J., Spreng, R.N., Cole, M.W.,

Christoff, K., 2018. Heterogeneity within the frontoparietal control network and its relationship to the default and dorsal attention networks. Proceedings of the National Academy of Sciences, 201715766.

Duncan, J., 2010. The multiple-demand (MD) system of the primate brain: mental programs for intelligent behaviour. Trends in cognitive sciences 14, 172-179.

Duncan, J., Owen, A.M., 2000. Common regions of the human frontal lobe recruited by diverse cognitive demands. Trends in neurosciences 23, 475-483.

Evans, A.C., 2013. Networks of anatomical covariance. Neuroimage 80, 489-504.

Fedorenko, E., Duncan, J., Kanwisher, N., 2013. Broad domain generality in focal regions of frontal and parietal cortex. Proceedings of the National Academy of Sciences 110, 16616-16621.

Fischl, B., Dale, A.M., 2000. Measuring the thickness of the human cerebral cortex from magnetic resonance images. Proceedings of the National Academy of Sciences 97, 11050-11055.

Fischl, B., Liu, A., Dale, A.M., 2001. Automated manifold surgery: constructing geometrically accurate and topologically correct models of the human cerebral cortex. IEEE transactions on medical imaging 20, 70-80.

Fischl, B., Sereno, M.I., Dale, A.M., 1999. Cortical surface-based analysis: II: inflation, flattening, and a surface-based coordinate system. Neuroimage 9, 195-207.

Gold, B.T., Balota, D.A., Jones, S.J., Powell, D.K., Smith, C.D., Andersen, A.H., 2006. Dissociation of automatic and strategic lexical-semantics: functional magnetic resonance imaging evidence for differing roles of multiple frontotemporal regions. Journal of Neuroscience 26, 6523-6532.

Gold, B.T., Balota, D.A., Kirchhoff, B.A., Buckner, R.L., 2005. Common and dissociable activation patterns associated with controlled semantic and phonological processing: evidence from fMRI adaptation. Cerebral Cortex 15, 1438-1450.

Gold, B.T., Buckner, R.L., 2002. Common prefrontal regions coactivate with dissociable

posterior regions during controlled semantic and phonological tasks. Neuron 35, 803-812.

Green, A.E., Cohen, M.S., Raab, H.A., Yedibalian, C.G., Gray, J.R., 2015. Frontopolar activity and connectivity support dynamic conscious augmentation of creative state. Human brain mapping 36, 923-934.

Hallam, G.P., Thompson, H.E., Hymers, M., Millman, R.E., Rodd, J.M., Ralph, M.A.L., Smallwood, J., Jefferies, E., 2018. Task-based and resting-state fMRI reveal compensatory network changes following damage to left inferior frontal gyrus. Cortex 99, 150-165.

Hallam, G.P., Whitney, C., Hymers, M., Gouws, A.D., Jefferies, E., 2016. Charting the effects of TMS with fMRI: Modulation of cortical recruitment within the distributed network supporting semantic control. Neuropsychologia 93, 40-52.

Hertrich, I., Dietrich, S., Ackermann, H., 2016. The role of the supplementary motor area for speech and language processing. Neuroscience & Biobehavioral Reviews 68, 602-610.

Hoffman, P., Jefferies, E., Ralph, M.A.L., 2010. Ventrolateral prefrontal cortex plays an executive regulation role in comprehension of abstract words: convergent neuropsychological and repetitive TMS evidence. Journal of Neuroscience 30, 15450-15456.

Humphreys, G.F., Lambon Ralph, M.A., 2017. Mapping domain-selective and counterpointed domain-general higher cognitive functions in the lateral parietal cortex: evidence from fMRI comparisons of difficulty-varying semantic versus visuo-spatial tasks, and functional connectivity analyses. Cerebral Cortex 27, 4199-4212.

Jefferies, E., 2013. The neural basis of semantic cognition: Converging evidence from neuropsychology, neuroimaging and TMS. Cortex 49, 611-625.

Jefferies, E., Lambon Ralph, M.A., 2006. Semantic impairment in stroke aphasia versus semantic dementia: a case-series comparison. Brain 129, 2132-2147.

Jung-Beeman, M., 2005. Bilateral brain processes for comprehending natural language.

Trends in cognitive sciences 9, 512-518.

Kanai, R., Rees, G., 2011. The structural basis of inter-individual differences in human behaviour and cognition. Nature Reviews Neuroscience 12, 231.

Kelly, C., Toro, R., Di Martino, A., Cox, C.L., Bellec, P., Castellanos, F.X., Milham, M.P., 2012. A convergent functional architecture of the insula emerges across imaging modalities. Neuroimage 61, 1129-1142.

Krieger-Redwood, K.M., 2012. An investigation of phonological and semantic control using TMS and fMRI. University of York.

Lambon Ralph, M. A., Jefferies, E., Patterson, K., Rogers, T.T., 2017. The neural and computational bases of semantic cognition. Nature Reviews Neuroscience 18, 42.

Lau, H.C., Rogers, R.D., Passingham, R.E., 2007. Manipulating the experienced onset of intention after action execution. Journal of Cognitive Neuroscience 19, 81-90.

Lerch, J.P., Worsley, K., Shaw, W.P., Greenstein, D.K., Lenroot, R.K., Giedd, J., Evans, A.C., 2006. Mapping anatomical correlations across cerebral cortex (MACACC) using cortical thickness from MRI. Neuroimage 31, 993-1003.

Lorch Jr, R.F., 1982. Priming and search processes in semantic memory: A test of three models of spreading activation. Journal of verbal learning and verbal behavior 21, 468-492.

Luders, E., Narr, K.L., Thompson, P.M., Rex, D.E., Woods, R.P., DeLuca, H., Jancke, L., Toga, A.W., 2006. Gender effects on cortical thickness and the influence of scaling. Human brain mapping 27, 314-324.

Mars, R.B., Klein, M.C., Neubert, F.-X., Olivier, E., Buch, E.R., Boorman, E.D., Rushworth, M.F., 2009. Short-latency influence of medial frontal cortex on primary motor cortex during action selection under conflict. Journal of Neuroscience 29, 6926-6931.

Mednick, M.T., Mednick, S.A., Mednick, E.V., 1964. Incubation of creative performance and specific associative priming. The Journal of Abnormal and Social Psychology 69, 84.

Mednick, S., 1962. The associative basis of the creative process. Psychological review 69, 220.Mollo, G., Karapanagiotidis, T., Bernhardt, B.C., Murphy, C.E., Smallwood, J., Jefferies, E., 2016. An individual differences analysis of the neurocognitive architecture of the semantic system at rest. Brain and Cognition 109, 112-123.

Moore-Parks, E.N., Burns, E.L., Bazzill, R., Levy, S., Posada, V., Müller, R.-A., 2010. An fMRI study of sentence-embedded lexical-semantic decision in children and adults. Brain and Language 114, 90-100.

Murphy, C., Jefferies, E., Rueschemeyer, S.-A., Sormaz, M., Wang, H.-t., Margulies, D.S., Smallwood, J., 2018. Distant from input: Evidence of regions within the default mode network supporting perceptually-decoupled and conceptually-guided cognition. Neuroimage.

Murphy, K., Birn, R.M., Handwerker, D.A., Jones, T.B., Bandettini, P.A., 2009. The impact of global signal regression on resting state correlations: are anti-correlated networks introduced? Neuroimage 44, 893-905.

Nichols, T., Brett, M., Andersson, J., Wager, T., Poline, J.B., 2005. Valid conjunction inference with the minimum statistic. Neuroimage 25, 653–660. https://doi.org/10.1016/j.neuroimage.2004.12.005

Noonan, K.A., Jefferies, E., Corbett, F., Lambon Ralph, M.A., 2010. Elucidating the nature of deregulated semantic cognition in semantic aphasia: evidence for the roles of prefrontal and temporo-parietal cortices. Journal of Cognitive Neuroscience 22, 1597-1613.

Noonan, K.A., Jefferies, E., Visser, M., Ralph, M.A.L., 2013. Going beyond Inferior Prefrontal Involvement in Semantic Control: Evidence for the Additional Contribution of Dorsal Angular Gyrus and Posterior Middle Temporal Cortex. Journal of Cognitive Neuroscience 25, 1824-1850.

Noppeney, U., Phillips, J., Price, C., 2004. The neural areas that control the retrieval and selection of semantics. Neuropsychologia 42, 1269-1280.

Patterson, K., Nestor, P.J., Rogers, T.T., 2007. Where do you know what you know? The

representation of semantic knowledge in the human brain. Nature Reviews Neuroscience 8, 976-987.

Rodd, J.M., Davis, M.H., Johnsrude, I.S., 2005. The neural mechanisms of speech comprehension: fMRI studies of semantic ambiguity. Cerebral Cortex 15, 1261-1269.

Rushworth, M., Hadland, K., Paus, T., Sipila, P., 2002. Role of the human medial frontal cortex in task switching: a combined fMRI and TMS study. Journal of neurophysiology 87, 2577-2592.

Schilling, C., Kühn, S., Romanowski, A., Schubert, F., Kathmann, N., Gallinat, J., 2012. Cortical thickness correlates with impulsiveness in healthy adults. Neuroimage 59, 824-830.

Seeley, W.W., Crawford, R.K., Zhou, J., Miller, B.L., Greicius, M.D., 2009. Neurodegenerative diseases target large-scale human brain networks. Neuron 62, 42-52.

Segall, J.M., Allen, E.A., Jung, R.E., Erhardt, E.B., Arja, S.K., Kiehl, K.A., Calhoun, V.D., 2012. Correspondence between structure and function in the human brain at rest. Frontiers in neuroinformatics 6, 10.

Snowden, J.S., Harris, J.M., Thompson, J.C., Kobylecki, C., Jones, M., Richardson, A.M., Neary, D., 2017. Semantic dementia and the left and right temporal lobes. Cortex.

Sormaz, M., Jefferies, E., Bernhardt, B.C., Karapanagiotidis, T., Mollo, G., Bernasconi, N., Bernasconi, A., Hartley, T., Smallwood, J., 2017. Knowing what from where: Hippocampal connectivity with temporoparietal cortex at rest is linked to individual differences in semantic and topographic memory. Neuroimage 152, 400-410.

Tamnes, C.K., Østby, Y., Fjell, A.M., Westlye, L.T., Due-Tønnessen, P., Walhovd, K.B., 2010. Brain maturation in adolescence and young adulthood: regional age-related changes in cortical thickness and white matter volume and microstructure. Cerebral Cortex 20, 534-548.

Thompson, R., Duncan, J., 2009. Attentional modulation of stimulus representation in human fronto-parietal cortex. Neuroimage 48, 436-448.

Thompson-Schill, S.L., D'Esposito, M., Aguirre, G.K., Farah, M.J., 1997. Role of left inferior prefrontal cortex in retrieval of semantic knowledge: a reevaluation. Proceedings of the National Academy of Sciences 94, 14792-14797.

Thompson-Schill, S.L., Swick, D., Farah, M.J., D'Esposito, M., Kan, I.P., Knight, R.T., 1998. Verb generation in patients with focal frontal lesions: A neuropsychological test of neuroimaging findings. Proceedings of the National Academy of Sciences 95, 15855-15860.

Tomita, H., Ohbayashi, M., Nakahara, K., Hasegawa, I., Miyashita, Y., 1999. Top-down signal from prefrontal cortex in executive control of memory retrieval. Nature 401, 699.

Tompkins, C.A., Scharp, V.L., Meigh, K.M., Fassbinder, W., 2008. Coarse coding and discourse comprehension in adults with right hemisphere brain damage. Aphasiology 22, 204-223.

Townsend, J.T., Ashby, F.G., 1983. Stochastic modeling of elementary psychological processes. CUP Archive.

Ulrich, M., Hoenig, K., Grön, G., Kiefer, M., 2013. Brain activation during masked and unmasked semantic priming: commonalities and differences. Journal of Cognitive Neuroscience 25, 2216-2229.

Valk, S.L., Bernhardt, B.C., Böckler, A., Trautwein, F.-M., Kanske, P., Singer, T., 2017. Socio-cognitive phenotypes differentially modulate large-scale structural covariance networks. Cerebral Cortex 27, 1358-1368.

van Gaal, S., Scholte, H.S., Lamme, V.A., Fahrenfort, J.J., Ridderinkhof, K.R., 2011. Pre-SMA gray-matter density predicts individual differences in action selection in the face of conscious and unconscious response conflict. Journal of Cognitive Neuroscience 23, 382-390.

Vatansever, D., Bzdok, D., Wang, H.-T., Mollo, G., Sormaz, M., Murphy, C., Karapanagiotidis, T., Smallwood, J., Jefferies, E., 2017. Varieties of semantic cognition revealed through simultaneous decomposition of intrinsic brain connectivity and behaviour. Neuroimage 158, 1-11.

Vitello, S., Warren, J.E., Devlin, J.T., Rodd, J.M., 2014. Roles of frontal and temporal regions in reinterpreting semantically ambiguous sentences. Frontiers in human neuroscience 8, 530.

Wagner, A.D., Paré-Blagoev, E.J., Clark, J., Poldrack, R.A., 2001. Recovering meaning: left prefrontal cortex guides controlled semantic retrieval. Neuron 31, 329-338.

Wei, T., Liang, X., He, Y., Zang, Y.F., Han, Z.Z., Caramazza, A., Bi, Y.C., 2012. Predicting Conceptual Processing Capacity from Spontaneous Neuronal Activity of the Left Middle Temporal Gyrus. Journal of Neuroscience 32, 481-489.

Whitney, C., Kirk, M., O'sullivan, J., Lambon Ralph, M.A., Jefferies, E., 2011. The neural organization of semantic control: TMS evidence for a distributed network in left inferior frontal and posterior middle temporal gyrus. Cerebral Cortex 21, 1066-1075.

Whitney, C., Kirk, M., O'Sullivan, J., Lambon Ralph, M.A., Jefferies, E., 2012. Executive semantic processing is underpinned by a large-scale neural network: revealing the contribution of left prefrontal, posterior temporal, and parietal cortex to controlled retrieval and selection using TMS. Journal of Cognitive Neuroscience 24, 133-147.

Worsley, K., Andermann, M., Koulis, T., MacDonald, D., Evans, A., 1999. Detecting changes in nonisotropic images. Human brain mapping 8, 98-101.

Worsley, K.J., Taylor, J., Carbonell, F., Chung, M., Duerden, E., Bernhardt, B., Lyttelton, O., Boucher, M., Evans, A., 2009. A Matlab toolbox for the statistical analysis of univariate and multivariate surface and volumetric data using linear mixed effects models and random field theory. NeuroImage Organisation for Human Brain Mapping 2009 Annual Meeting, p. S102.

Xia, M., Wang, J., He, Y., 2013. BrainNet Viewer: a network visualization tool for human brain connectomics. PloS one 8, e68910.

Yeo, B. T., Krienen, F.M., Sepulcre, J., Sabuncu, M.R., Lashkari, D., Hollinshead, M., Roffman, J.L., Smoller, J.W., Zöllei, L., Polimeni, J.R., 2011. The organization of the human cerebral cortex estimated by intrinsic functional connectivity. Journal of neurophysiology 106, 1125-1165.

Zhang, Y., Brady, M., Smith, S., 2001. Segmentation of brain MR images through a hidden Markov random field model and the expectation-maximization algorithm. IEEE transactions on medical imaging 20, 45-57.